To appear in *Advanced Robotics*
Vol. 00, No. 00, April 2018, 1–19

FULL PAPER

Effects of Passive and Active Joint Compliance in Quadrupedal Locomotion

M. Mutlu[a,b]*, S. Hauser[a], A. Bernardino[b], A. J. Ijspeert[a]

[a] *BIOROB EPFL, Lausanne, Switzerland*;
[b] *Vislab IST, Lisbon, Portugal*

(*30. November 2017*)

Compliance of the body has a crucial role on locomotion performance. The levels and the distribution of compliance should be well tuned to obtain efficient gait. The leg stiffness changes significantly even during different phases of a single gait cycle. This paper presents an experimental study on different passive and active limb compliance configurations. Each configuration is tested on flat, rough and inclined-rough surfaces, to analyze locomotion performance in diverse conditions. As the active compliance mechanism, Tegotae-based control is selected. Even though active compliance is not its primary use, we show that the Tegotae rule presents intriguing features that have potential to boost gait performance in various scenarios.

Keywords: locomotion, compliance, Tegotae, stiffness, passive compliance, active compliance

1. Introduction

Quadrupedal animals exhibit great adaptability to changing environment conditions during locomotion. Adaptation can be in the form of reflexive actions, gait change or muscle stiffness modulation. While reflexes and gait transitions drastically alters locomotion characteristics, muscle stiffness modulation usually improves performance without completely changing the locomotion type. The performance criteria can include energy efficiency, speed, precision, accuracy etc.. For instance, real animals move in an energy efficient way [1]. Different performance demands yield different optimal muscle stiffnesses.

Compliance is a crucial characteristic in legged animal locomotion. All parts of the musculoskeletal system of a body, muscles, tendons, tissue, skin, bones etc., exhibit different levels of compliance. The effects of compliance greatly vary on the momentary task or activity. It has the potential to add robustness to stiff/brittle structures, is able to store and release energy and can help to reduce peak forces e.g. when an impact is experienced. In order to profit from such properties, it is important to note that in most cases compliance needs to be well-tuned to obtain a desired effect.

In locomotion, compliance is thought to play a key-role in many aspects from safety and gait stabilization to energy efficiency and dynamic gaits (e.g. [2]). It is unclear however, which kind of compliance acts on which aspects of locomotion and how to quantify potential benefits. For instance, according to [3], compliant legs are essential to obtain the basic walking mechanics in bipedal human locomotion. A widely used approach is adding a passive compliance as demonstrated in [4–7]. A pragmatic extension to passive compliance is the capability of tuning stiffness using hardware approaches either during the locomotion or even during a single step cycle [8–10] with variable stiffness actuators.

*Corresponding author. Email: mehmet.mutlu@epfl.ch

Elastic, spring-like materials are not the only way to achieve compliance. Using proximal sensors and an active control, it is possible to model virtual spring effects and integrate into motor servo control, described as proxy-based sliding mode in [11]. Another use of virtual springs during quadrupedal locomotion is explained in [12]. Impedance control through controlling torque is also widely used to adjust compliance, e.g. [13] shows an implementation on quadrupedal locomotion. Force sensors on the feet can be incorporated to achieve actively compliant locomotion [14] in a morphologically rigid robot. In a recent study [15], the authors propose compliant locomotion through Tegotae-based, sensory feedback driven control where phase coupling of leg oscillators emerge from robot-environment interaction. By incorporating machine learning to footstep planning [16, 17] it is also possible to achieve adaptation to highly rough terrain.

The robots that use the Tegotae-based control scheme have usually been reported to have series elastic elements on legs [18]. The Tegotae scheme can clearly generate different gaits (trot, bound, gallop etc.) and the passive compliance of the leg has a modulating role. [15] declares that a lower level of active-stiffness results in less Tegotae (good/useful feedback) in robot-environment interaction and steady state locomotion may be severely degraded for very low stiffness values.

Despite all previous works emphasize the importance of compliant legs, they cover only limited aspects. In particular, they lack the analysis of compliant locomotion in rough terrains. Moreover, there are limited previous studies on the combined effect of passive and active compliance on locomotion performance. We could not find any study qualitatively evaluating the relationship of different levels of passive compliance and the Tegotae based control.

The driving force this paper is the increasing need to understand role of both passive and active compliance better in quadrupedal locomotion. To this end, a compliant modular quadruped robot has been designed using low-budget off-the-shelf components. The robot is highly customizable and fast to reconfigure which enables a wide set of experiment possibilities involving morphological changes. The goal of the paper is to answer a set of questions which are

(1) How does the passive compliance of legs affect quadrupedal robot locomotion?
(2) Can having asymmetric passive compliance on fore and hind limbs increase the performance of locomotion?
(3) Is it possible to boost adaptation of the robot to its environment using active compliance?
(4) Does active compliance and passive compliance cooperate well or destruct each other's contributions?
(5) Do results scale up to different terrains?

Contributions of the paper are three-fold: (i) a comprehensive and systematic experimental analysis of quadrupedal locomotion on various surfaces with passive leg compliance; (ii) a quantitative analysis on combination of Tegotae-based control and passive leg compliance under changing compliance levels; (iii) the first study of Tegotae-based control of a quadruped robot on rough terrain.

The rest of the paper is organized as follow. Details of the implementation and experiments are given in Sec. 2 and Sec. 3 respectively. Analysis and findings from the data are explained in the Sec. 4. Finally, the paper is concluded in Sec. 5.

2. Methods

2.1 *Hardware platform*

This study is conducted on a simple yet dynamically rich quadrupedal morphology. The robot consists of a rectangular body (39 cm x 23.5 cm). The overall structure of the robot can be seen in Fig. 1.a. Each limb has 2 degrees of freedom (DOF) where the upper leg (L1) is 79mm and the lower leg (L2) is 110mm. The motion of the limbs is constrained to the sagittal plane. Each hip joint is powered by a Dynamixel RX-28 servo motor and each knee joint is powered

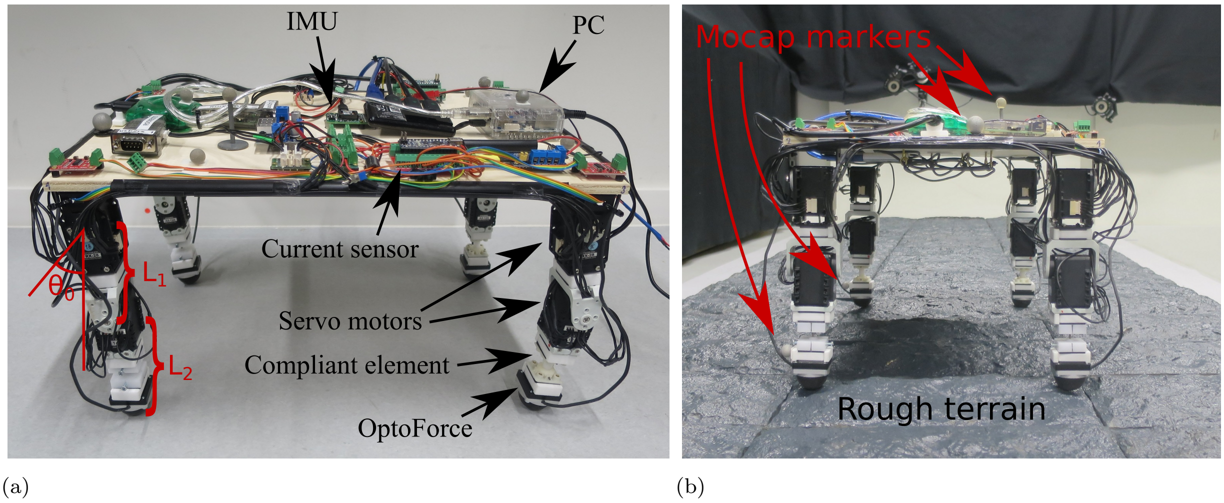

Figure 1. (a) The quadrupedal robot consists of various on-board sensors and has an embedded PC to collect all the data and handle the high level control. (b) The control PC can get the data from the external tracking system through Wi-Fi. All data is collected on the same PC to ensure synchronization across various sensors.

by a Dynamixel AX-12A. In a preliminary study [19], it is shown that the proximal parts of the limb should have higher compliance compared to the distal parts. Hence, the proximal hip part of the leg is directly connected to the lower (distal) leg without any compliant elements in between. However, lower limbs are extended with easily changeable "compliant elements" which can have different mechanical properties such as height, spring stiffness, weight etc.. In this study the different tested elements are designed to have the same dimensions and only the spring stiffness is varied. They are rigid elements made out of Polyoxymethylene (POM) rods and two types of compliant elements made out of super-elastic Nitinol wire with diameters of d =1.5 mm (further called "soft") and 2 mm (further called "hard") with corresponding flexural stiffnesses 2.3 Nm/rad and 7.3 Nm/rad; torsional stiffnesses 1.75 Nm/rad and 5.54 Nm/rad [20]. The three different elements and the quick locking mechanism are shown in Fig. 2. The quick lock mechanism eliminates the need of extra tools to exchange compliant elements and considerably accelerates the exchange process.

The robot is equipped with an embedded PC to collect sensor data and control servo motors. The detailed list of on-board components is as follows:

- *Dynamixel RX-28* servo motors (4x)
- Interchangeable passive elements (4x)
- *Dynamixel AX-12* servo motors (4x)
- *Optoforce OMD-30-SE-100N* 3D-force sensors (4x)
- *ODROID-XU4* embedded control pc
- *INA169* DC current sensor
- *Xsens MTi-3 AHRS* IMU
- *USB2Dynamixel* communication bus converter (2x)
- *LM2596S* (12V) DC Voltage regulator

The servo motors are used for joint angle control and have encoders that feed back their position. The current sensor measures the total current going to the motors at 1500 Hz. The current sensor has an intermediary Arduino board to send the data to the PC. The robot is powered externally through a tether from a DC voltage source. Since the source voltage is the same, the current reading directly correlates to the power demanded by motors during locomotion. Force sensors give 3D ground reaction force information on each foot which is essential for the Tegotae control scheme. The IMU has a 3-axis accelerometer, a 3-axis gyro and a 3-axis magnetometer. It is used for recording acceleration and rotational velocity of the robot's body at 100 Hz during locomotion. Due to drifts in the IMU, the global pose of the robot is tracked with an external

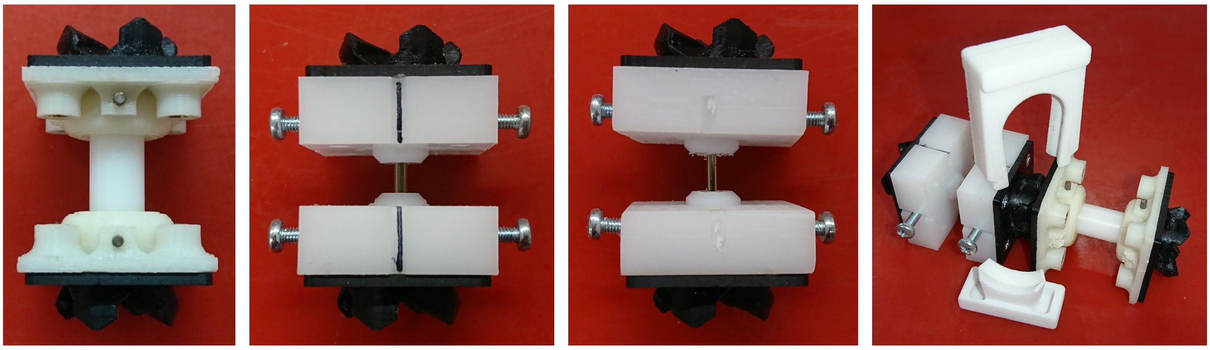

(a) (b) (c) (d)

Figure 2. Three different elements with the same dimensions have been used in this study: (a) rigid Polyoxymethylene (POM), (b) super elastic nitinol wire with 2mm and (c) 1.5mm diameter. (d) A locking mechanism has been designed which eliminates need for tools for the change of elements and enables quick change of elements. The mechanism consists of two interlocking pieces that wrap around the connection joint.

motion capture (MoCap) system (Fig. 1.b). The MoCap data is also streamed to the robot's on-board PC to ensure synchronization across different data sources. Thus, all data frames are timestamped with the same clock and they are inherently synchronized.

2.2 *Gait generation*

Quadrupedal animals can walk or run in a great variety of ways. In this study we picked the "trot" gait for our analysis since it is one of the most energy efficient quadrupedal gaits that is observed on many quadrupedal animals during long journeys [21]. Moreover, trot is a switching gait from walking to fast galloping. Hence, it has rich dynamical characteristics, but does not demand very high actuator power. In this study, two different types of controllers will be tested: (i) open loop control (forced to trot) and (ii) Tegotae-based closed loop control.

2.3 *Foot trajectory*

In this study, the role of locomotion controller is coordinating the phase of a gait cycle. However, the desired trajectory that a foot tracks is designed as a predefined cyclic motion. The parameters of the foot trajectory, swing amplitude and swing height, are optimized using Particle Swarm Optimization (PSO) in a simulation environment to yield faster speed for a given constant locomotion frequency. The shape of the foot trajectory is set to be two different elliptic arcs during stand and swing phases with maximum 1.5 cm foot clearance ($h_{sw} - h_{st}$) as illustrated in Fig. 3. The mid stance phase is marked as p_2, mid swing phase is marked as p_4 and stance-swing switching moments are marked as p_1 and p_3. For the inclined surface locomotion, an offset $\theta_0 = 0.1$ rad (5.7 deg) is added to the hip angle to shift the center of mass slightly forward. Details of the implemented foot trajectory are further explained in [22].

2.4 *Open loop CPG-based control*

Legged locomotion can be achieved to some extend in an open loop control scheme, although the expected robustness of the gait would be low. Open loop control is chosen to form a baseline in this study. The steady-state locomotion is a cyclic motion such that each limb i is at a specific phase $\phi_i(t)$ of the cycle at the given time t.

In this particular implementation, each leg's motion is modeled as a phase-oscillator to steer the system into a desired limit cycle [7, 23–25]. Leg oscillators are coupled to each other in lateral and axial fashion. The phase of each limb i is described by the set of coupled differential

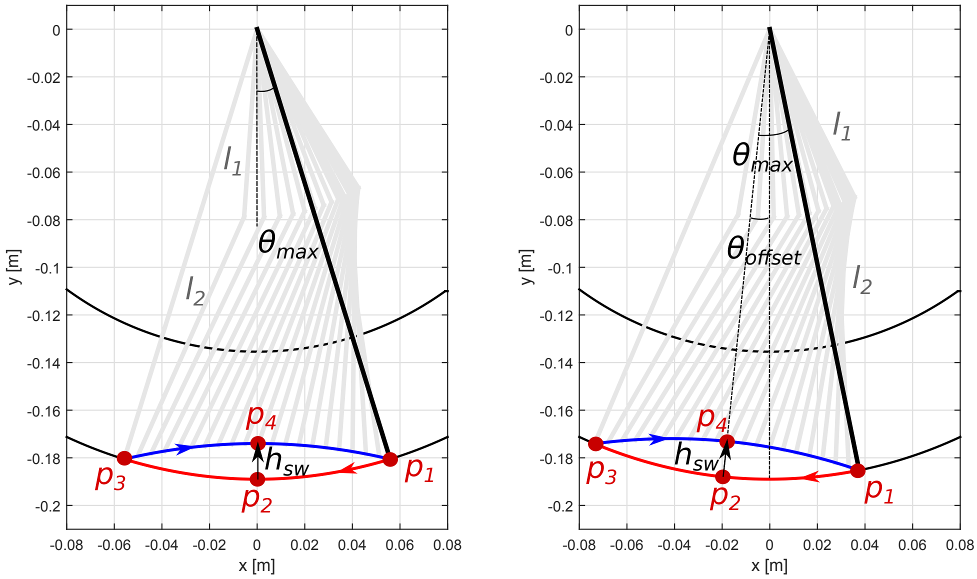

(a) (b)

Figure 3. (a) The designed foot trajectory when the hip is fixed and foot freely moves in the air. Blue elliptic arc shows the swing phase and the red one shows the stance phase. Limits of the workspace is shown with black arcs. Parameters defining the gait are hip angle maximum extension ($\theta_{max} = 0.3rad$), height difference from swing phase mid point to fully stretched leg ($h_{sw} = 15mm$) and height difference from stance phase mid point to fully stretched leg ($h_{st} = 0mm$). (b) As an inclination compensation, an offset angle ($\theta_{offset} = 0.1rad$) is added to the hip angle.

equations given as

$$\dot{\phi}_i = 2\pi f + \sum_j w_{ij} \, \sin(\phi_j - \phi_i - \psi_{ij}) \tag{1}$$

where ϕ denotes the phase of an oscillator, f is the gait frequency and ψ is the desired phase difference between two oscillators. The coupling terms adjust the phase update of each oscillator, according to the phase of the neighbors ϕ_j, desired phase shift ψ_{ij} between limbs i and j, and the weight of the coupling w_{ij}. The phase update rule given in Eq. 1 brings the system - starting from any arbitrary initial conditions - to a desired limit cycle after an initial transient phase. At steady state, the locomotion frequency is constant. First, the phase is propagated which then is used to calculate the actual joint commands using the desired Cartesian foot trajectory and inverse kinematics. In other words, ϕ is given to hip and knee local PID controllers as the set-point after conversion to joint angles. ϕ is integrated within the controller and it is independent of the real leg phase measured by encoders. A separate feedback term that measures real leg angles could have been added to the Eq. 1. But, open loop control is chosen as a baseline to keep compliance experiments isolated from effects of feedback. Due to bandwidth limitations of the servo motors, open loop gait frequency is set to 0.5 Hz throughout all experiments.

2.5 *Tegotae-based control*

In the open loop control, coordination of the legs depends on hard-coded couplings between the oscillators. On the other hand, Tegotae-based control has no explicit leg coordination and oscillators are coupled indirectly through sensory feedback. All phase oscillators are independent. However, the Tegotae method is making use of local force feedback and the phase oscillators still naturally converge to a synchronized behavior due to the dynamic robot-environment interaction. In this study the implemented Tegotae scheme is similar to the one explained in [26]. The phase equations of limb oscillators are given as

$$\dot{\phi}_i = 2\pi f + s\, N_i\, \cos(\phi_i) \tag{2}$$

where N_i is the z axis reading of the force sensor which corresponds to the axial normal force applied to ith leg by the ground and s is the Tegotae attraction coefficient. The equation implies that whenever there is a normal ground reaction force on a foot, a phase attraction is created towards the mid-stance phase. More visually, ϕ gets attracted towards p_2 during the stance phase shown as red arc from p_1 to p_3 in Fig. 3. Amount of attraction depends on the normal ground reaction force. Another expectation is that on a rough terrain, robot will not exhibit periodic body oscillations which will lead to slightly different phase changes at each gait cycle and the Tegotae-based control is expected to introduce an exploratory stepping behavior.

Hypothesis 1 (H1)**.** *Tegotae-based control will improve rough terrain locomotion performance thanks to its exploratory nature.*

In [15], there are two Tegotae rules; one modulating the phase and the other one modulating the proportional constant (K_P) of the local PID controller. Changing K_P is not always easy in real hardware. Most of the local PID controllers are not designed for seamless operation in constantly changing parameters especially due to involved setting delays. It is also the case for the hardware presented in this work. Hence, only the conventional Tegotae rule is considered. Nevertheless, the conventional Tegotae rule can be considered as a set-point control scheme and it has dampening and exploratory characteristics and imitates a compliant control.

3. Experiments

This paper is primarily based on an experimental study. Main research questions of this paper were posed in Sec. 1. Our strategy to tackle each question can be summarized as follows:

(1) Add series passive compliant elements to all of the legs.
(2) Use elements having different compliance on fore and hind limbs.
(3) Implement Tegotae-based control and observe if it introduces any advantages over passive compliance.
(4) Test closed loop active controller with different leg compliances.
(5) Repeat experiments for different surface conditions.

To address all of these questions, experiments need to involve analyzing various hardware configurations using open and closed loop controllers on different surface conditions. Our approach is a comprehensive exhaustive systematic search where only one parameter is changed at a time. At each different scenario, the robot runs more than 10 steps in steady-state and the last 10 steps of each run are taken for analysis. The rest of this section elaborates the details of the followed procedures.

3.1 *Passive compliance*

The passive elements tested in this study are the same as the ones used in [19]. The rigid element sets a baseline for the other compliant elements. The only upgrade is the locking mechanism which does not get loose during the locomotion and has considerably less backlash compared to the one used in [19]. It is important to note that the robot itself has an intrinsic compliance arising from body elasticities, motor and connector backlashes and low level servo control errors. Hence, even the case with the rigid elements has a hard-to-model parasitic compliance. The other elements introduce significant compliance on the lower limb only.

The selection of compliance distribution is empirical. The main aim is to observe effects of relative compliance. There exists $3^4 = 81$ different distributions using only 3 compliance levels on 4 limbs. Left-right of the robot is always kept symmetric as in most healthy quadrupedal animals. When the left/right symmetry is considered, number of possible compliance distributions reduce to $3^2 = 9$. Most of the quadrupedal animals also have stronger and bigger hind limbs then fore limbs. Thus, the distributions where hind limbs are softer than fore limbs (3 cases) are discarded. In this study 5 different compliant element distributions are tested: (i) "all limbs rigid" (practically no bending), (ii) "all limbs hard" (low to moderate bending), (iii) "all limbs soft" (moderate to high bending), (iv) "fore limbs hard / hind limbs rigid", (v) "fore limbs soft / hind limbs rigid".

"Fore limbs soft / hind limbs hard" distribution is intentionally left out. Because, "fore limbs complaint / hind limbs rigid" cases (4^{th} and 5^{th} distributions) are expected to give similar trend with the excluded case. Moreover, initial tests revealed that robot has more troubles with soft leg compliances compared to harder/moderate distributions. Hence one of the visually not very promising distributions is not selected for further experiments to reduce the total number of runs.

3.2 *Tegotae-based active compliance*

Tegotae control is demonstrated to have the capability to generate rich set of locomotion modes without setting any coupling between leg oscillators by modulating only a single variable (s). Moreover, Tegotae can adapt the gait to asymmetrical morphology changes too [22]. Hence it may not be a perfectly matching condition to compare open loop and Tegotae control since Tegotae may not always stay in trot mode. In order to close the difference gap, we have initialized the gaits controlled by Tegotae in trot. We also set a single value of Tegotae attraction coefficient ($s = 0.3$) which is experimentally checked to converge to trot gait at steady-state when locomoting on flat surface and most of the other cases. Due to its randomness, it is not possible to guarantee the steady-state trot convergence on the rough terrain. However, rich response characteristics of the Tegotae control make it even more interesting and worthy to study as an active compliance source.

3.3 *Experiment terrain*

Since Tegotae control is fundamentally based on the robot-environment interaction, different surface conditions are included in the study.

3.3.1 Flat surface, no inclination:

The flat surface with no inclination constitutes the baseline for the different surface types, because gait cycles are consistently repetitive and it is easier to observe steady state behavior particularly for the Tegotae control This surface type is the most commonly used one for the Tegotae experiments. Hence, it can be used as a bridge between other studies and our study.

3.3.2 Rough surface, no inclination:

A rough surface of 3 m x 1 m size is made out of house decoration tiles. The tiles are painted with spray paint to obtain the surface seen on Fig. 1.b because the original white color was too reflective under the motion capture system. The roughness consists of valleys and peaks having approximately 1 cm and maximum 2 cm height difference. Such roughness introduces stochastic perturbations to the robot's locomotion in the form of slippage or getting stuck. A robust locomotion is expected to perform well on the rough terrain.

3.3.3 Rough surface, 3 deg *uphill inclination:*

The final experiment surface is the 3 deg inclined version of the same rough terrain. The robot walked uphill during the tests. Uphill conditions are even more challenging since the gravity is against the locomotion direction.

In summary, we exhaustively tested all different conditions. Therefore, the experiment set consists of

$$5 \text{ (compliant element distribution)} * 2 \text{ (open and closed loop control)} * 3 \text{ (surface types)} = 30$$

runs.

4. Results and Discussions

This section presents the analysis of the data collected during the experiments as well as our observations and comments on the data. Quantifying the locomotion performance is done by introducing various metrics calculated by using logged data. Furthermore, qualitative gait symmetry analysis is presented to illustrate locomotion modes emerging from different leg compliance levels as well as the Tegotae-based rule. Finally, more insights are given about the Tegotae-based control on various surfaces. The answers to the questions posed in Sec. 1 can be found distributed throughout sections 4.2, 4.3, 4.4 and 4.5. Answers are not given in a list to keep the coherence of the text. However, visual marks such as $(A\#)$ are added around the relevant text to clarify our answers for the reader.

4.1 *Performance metrics*

Quantifying performance of locomotion is a challenging task as there are different perspectives to look at the same data and some of those approaches can be biased or not as important as others. In order to be as fair and rigorous as possible, many different performance metrics have been proposed. They can be grouped in two subgroups: (i) conventional metrics such as speed, cost of transport, power consumption etc., and (ii) stability of locomotion metrics to evaluate how much the body oscillated during the locomotion, i.e. how much it deviates from the horizontal plane.

4.1.1 Stride length (l_s):

The foot trajectory is the same for all of the experiments. However, the stride length is expected to change for different configurations because of slippage and the robot getting stuck. Having long strides without getting stuck is a desired locomotion criteria. This metric is calculated as

$$l_s = d_t/N_s \tag{3}$$

where d_t is the total distance taken in 10 steps and N_s is the number of steps (fixed to 10 in this study).

4.1.2 Experiment time for 10 steps (t_e):

By the definition of Tegotae, it has power to suppress or advance the gait phase. So, taking 10 steps always takes the same amount of time in open loop locomotion whereas the actual time needed to perform 10 steps with the Tegotae control varies around the gait period $(1/f)$. Hence, we report the time Tegotae-based control needs to take 10 steps. This metric is reported for the completeness and further used to calculate average speed. It is important to note that taking 10 steps within less time does not necessarily mean faster locomotion since actual stride length can change due to foot slipping or getting stuck even though the desired foot trajectory is the same for all experiments.

4.1.3 Average speed (v_a):

Although the stride length l_s is correlated with the average speed v_a, there can be differences since the experiment time for the Tegotae control is not fixed, i.e.:

$$v_a = d_t/t_e \tag{4}$$

Average speed is one of the most reported locomotion metrics in the literature since many researchers are trying to make faster robots.

4.1.4 Average power consumption (P_a):

The current demand for the locomotion is among the logged measurements. Motors are powered using a fixed DC voltage source. Hence the total power consumption for the experiment is

$$P_a = \frac{V_{DC}}{t_e} * \int_0^{t_e} I(t)dt \tag{5}$$

where $V_{DC} = 18$ V. Power consumption is a widely used metric in robotics because it has implications on the battery size and operation time of a robot.

4.1.5 Cost of transport (CoT):

The cost of transport evaluates the power efficiency of the locomotion and is calculated as

$$CoT = \frac{P_a}{m * g * v_a} \tag{6}$$

where m is the mass of the robot ($m = 2.25$ kg) and g is the gravitational constant. CoT is also one of the most common locomotion metrics in the literature and it gives the operation cost of the robot to move from point A to B.

4.1.6 Control tracking error (e):

We log the actual motor angles read from encoder and desired joint angles. The control error e is simply the mean (per actuator) of the absolute value of the difference of the setpoint and the actual motor angle. Setpoint tracking capability is a feature of the local controller, hence expected to be invariant throughout experiments since weight does not change. However, when the high level control input is very high or when motors are blocked, actuators may have higher setpoint tracking error. Lower local control errors indicate the robot is at least moving in a desired way and not getting stuck.

4.1.7 Average acceleration (a_a):

This metric and the following ones are related with the smoothness (oscillation amount) of the body motion during locomotion. A more oscillating locomotion may not necessarily be less stable than a more flat one. However, it is an indicator of the energy efficiency. We consider lower accelerations to be potentially better gaits. The average acceleration is simply the mean value of all acceleration vector's Euclidean norms logged during the locomotion.

4.1.8 Average rotational velocity (ω_a):

The IMU gives rotational velocity with respect to each axis in 3D. Total rotational velocity ω_a is calculated the same way as the acceleration and it relates to the stability of the body too.

4.1.9 Force fluctuations (σ_f):

The axial force fluctuation is calculated as

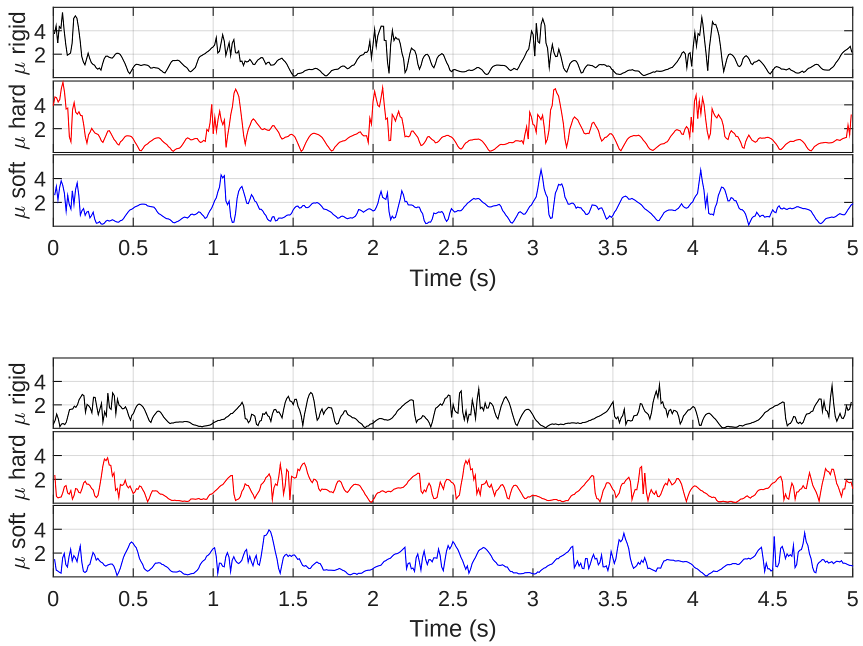

(a)

(b)

Figure 4. Motion based motion blur metric (MMBM, or shortly μ) values during 2,5 gait cycles when the robot is equipped with different compliant elements and walking on flat surface with (a) open loop and (b) Tegotae control. Higher metric values correspond to more blurry images. Hence, lower values are considered to be better for the locomotion.

$$\sigma_f = \sum_{i=1}^{4} \sigma_i \tag{7}$$

where σ_i is the standard deviation of the norm of (3D) data collected by the OptoForce sensors during the experiment. This metric is correlated with the amplitude of foot touchdown impacts. Higher impacts will usually result in higher σ_f values. High impacts can also deteriorate sensor readings and usually they are undesired in robotics unless high impacts are needed for a specific task.

4.1.10 Average motion blur (μ_a):

In order to enrich our analysis, we are adding a (Self) Motion-based Motion Blur Metric (MMBM, in short μ) which estimates the average motion blur of images caused by rotational motion of the robot's body if there was a fixed camera mounted on the robot's body. High levels of motion blur causes a loss of high frequency information on images and it is usually considered as an undesired artifact for further processing of images. The detailed explanation of the metric is given in [27]. This metric is calculated using only rotational velocity and camera parameters. As a result, it is highly correlated with the gyroscope data, but takes into account the image formation and the camera model. The variation of μ is similar to ω_a, but, they are different. The difference of the two metrics is more pronounced when the camera roll becomes the dominant motion. A MMBM value is calculated for each gyroscope data. An illustrative example is given in Fig. 4 where MMBM values during 2.5 gait cycles are depicted. Higher values of the metric corresponds to higher motion blur levels if an image is captured at that time instance. Hence lower average MMBM value is considered to be better for legged locomotion. μ_a is the mean of all MMBM samples collected during the locomotion. As seen in the plot, Tegotae-based control yields lower expected motion blur levels at peak points.

4.1.11 Chance to capture sharp images ($\mu_{\%}$):

MMBM can detect very blurry images before any image processing. This information can be used to selectively capture images when MMBM is low and discard images when MMBM is high. Even though the images can get extremely blurry at some phases of the gait and has higher MMBM average (μ_a), if there are long periods of low MMBM value, such a gait can also be useful for computer vision applications. This final metric is defined as

$$\mu_{\%} = \frac{n_s * 100}{n * N_s} \tag{8}$$

where n_s is the number of MMBM samples smaller than a predefined threshold (selected as 1 in our case) and n is the total number of MMBM samples. Camera motion blur related metrics are not very commonly used in the literature of robotic locomotion and they are quite task specific since they relate to image capturing quality on mobile cameras. However, we believe that it is another way to look at the locomotion performance and they enrich the locomotion analysis.

4.2 *Overall results*

The performance metrics explained in the previous subsection are calculated for all of the experimental data and the results are presented in Fig. 5. The axes in the spider plots have been reversed in necessary cases such that outer (from center) values indicate better locomotion performance in accordance with the defined metrics. Furthermore, all of the axes have the same range across different plots and their range is scaled and normalized such that the minimum metric value is always very close to the center and the maximum metric value is at the outer limits of the spider plot. Therefore, the area of each spider plot gives an idea about how good the performance is. However, it is important to note that under real conditions, different axes have different importances, thus the area of the spider plot is not an absolute classification criteria for any locomotion task. It is rather up to the reader's interests and intentions to choose and weight desired metrics for a performance evaluation. It is also important to note that very small metric value differences between different experiments may not be absolute indicator. The experiment time was limited to 10 gait cycles and especially on rough surface, error margins are expected to be higher due to randomness of the contact points.

The flat and rough terrain results show two major differences between open loop and Tegotae control: (i) Tegotae control takes longer t_e (experiment time for 10 steps) than the open loop control, but, (ii) the tracking error e resulting from the Tegotae control is less than the open loop e. ($A5$) Similar observations also hold for e on inclined surface locomotion. But, the difference of e between open loop and Tegotae control is less pronounced during inclined surface locomotion. An interesting observation is that t_e in Tegotae control is getting less than the open loop case on the inclined surface. The shortest t_e case occurs with the soft fore / rigid hind limb compliance on inclined surface. The reason is that the force on the z axis of the force sensor is changing direction. Fig. 6 shows right fore leg, the ground reaction forces, force sensor orientation as well as the sensor tip point during the mid-stance instance in rigid and soft fore/rigid hind compliance configurations on inclined rough terrain. The leg can be bent beyond the natural range when the compliance is too soft.

Another interesting observation is that the Tegotae control seems to have multiple benefits on both rough 0 deg and 3 deg inclined terrains. ($A3$ & $A4$) First of all, it has a tendency to decrease the cost of transport. Additionally, the metrics related with the stability of the robot (a_a, ω_a, e, μ_a etc.) are indicating the performance increase. Finally, the whole area that is covered by the spider plots also increase from open loop gaits to Tegotae control. That is a significant outcome indicating the Tegotae rule can boost locomotion performance on rough terrain, thus hypothesis **H1** is validated. It can also be concluded that introducing passive compliance to a robot having Tegotae-based control improves locomotion performance as long as compliance is

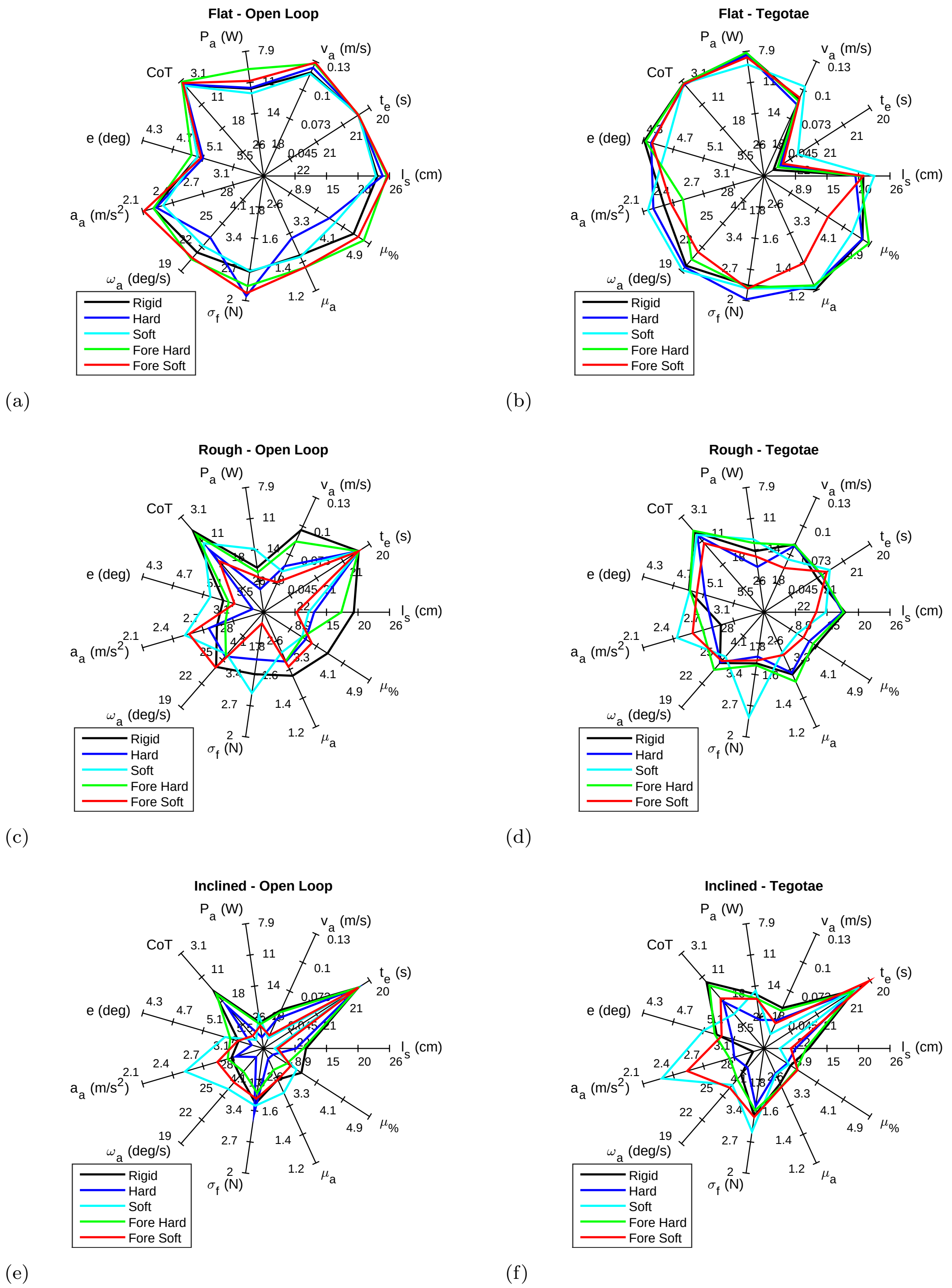

Figure 5. Evaluation of the proposed metrics for all of the experiments. The data is divided into 6 spider plots illustrating (a) flat terrain / open loop control, (b) flat terrain / Tegotae control, (c) rough terrain / open loop control, (d) rough terrain / Tegotae control, (e) inclined rough terrain / open loop control, (f) inclined rough terrain / Tegotae control. Each plot is showing all of the tested compliance distributions: (i) all rigid elements (practically no bending), (ii) all hard elements (low to moderate bending), (iii) all soft elements (moderate to high bending), (iv) fore limbs hard / hind limbs rigid elements, (v) fore limbs soft / hind limbs rigid elements.

within favorable range.

In terms of the compliance distribution, there is no single outstanding observation dominating for all runs. But, some of the distributions perform better under specific conditions. (A1) This is an expected result since this work tries to answer a broad range of questions. As there is no single algorithm to solve all problems, there is no perfect compliance distribution to satisfy

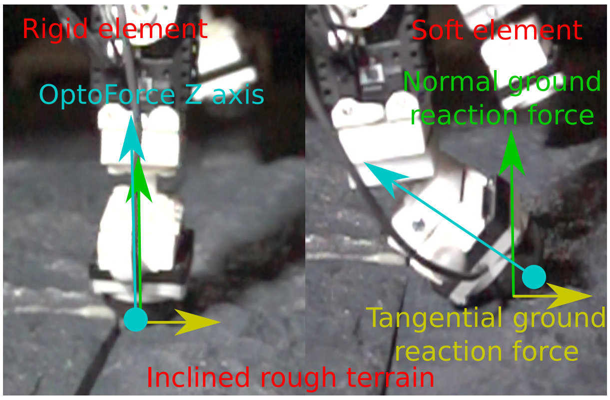

Figure 6. The ground reaction force and the orientation of the force sensor mounted on the foot. When the compliance is very low the bending can reach quite high and unnatural looking levels.

different goals. It is still possible to infer that fore hard / hind rigid case has better performance over all hard distribution. Which points out that asymmetric fore and hind limb compliance has potential to improve locomotion performance

The experimental data is presented as a comprehensive set without hiding some aspects that may seem insignificant in the first look. However, we believe that demonstrating invariance of certain metrics is as important as finding drastic correlations. Thanks to the completeness of the experiments, a wide range of readers can find even a subset of all results useful for their own designs.

4.3 *Feet trajectories*

During the trot, two legs should be in the stance phase while the other two should be in the swing phase. However, our robot does not have active feet controlled from the ankle and only has passive spherical feet. As a result, the robot has only two points rather than 2 surfaces in real quadrupedal animals, touching the ground at most of the times. Thus, the robot dynamics exhibit unstable, inverted-pendulum-like, behavior and one of the swing phase legs sometimes prematurely touch to the ground to form dynamically stable tripod (unnatural for animals). Even though, the center of mass is approximately at the geometric center of the robot, for all of the open loop gaits the tripod is formed by two hind limbs and a fore limb. Even when one of the swing phase legs touches the ground, the majority of the weight is still carried by the stance phase legs. In order to capture such behaviors, right feet trajectories are recorded during flat terrain experiments. Fig. 7 gives the fore and hind limb trajectories for all uniform compliance distributions when locomoting on the flat surface. It is clear that the hind leg is always dragging. ($A2$) However, Tegotae control is trying to balance that instability and trying to bring the system to more uniform swing/stance phases. Previously, it was reported that Tegotae rule can fight against introduced morphological asymmetries and tries to bring the locomotion to more symmetrical regime [22]. Similarly, we re-validate that Tegotae rule tries to overcome locomotion asymmetries. Furthermore, we observe cues to extend that hypothesis to include asymmetries arising from the locomotion surface.

4.4 *Phase vs compliance in Tegotae-based control*

The time evaluation of the phase gives important clues about the locomotion in Tegotae control. The phase of the limb oscillators when the robot is controlled with the Tegotae rule is given in Fig. 8. The figure displays three different runs with different uniform compliant elements. For each run, both right (fore and hind) limbs' phases are plotted. More stiff legs can have higher interaction forces and we observe that phase delay is increased. This observation is also consistent with the literature.

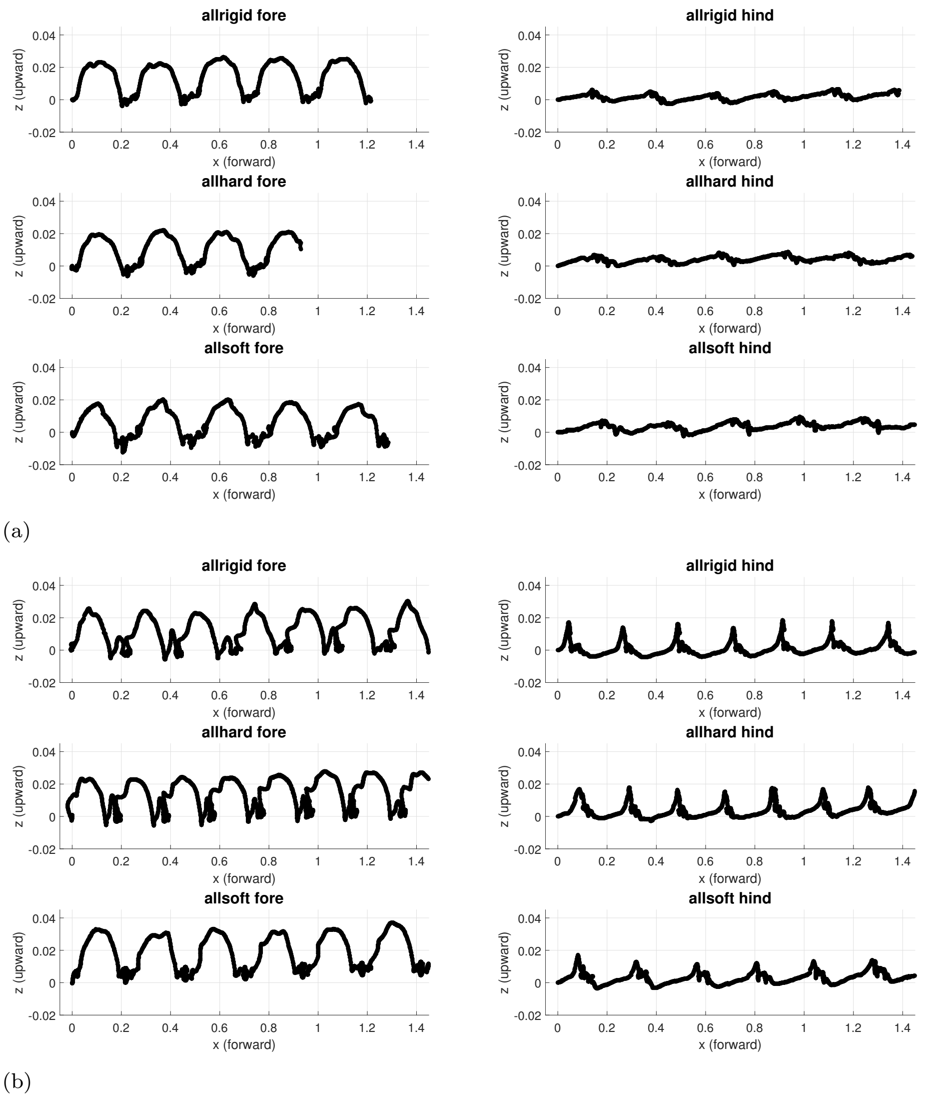

Figure 7. Foot trajectories during locomotion on the flat surface, using different uniform compliance when the robot is controlled with (a) open loop or (b) Tegotae based controllers.

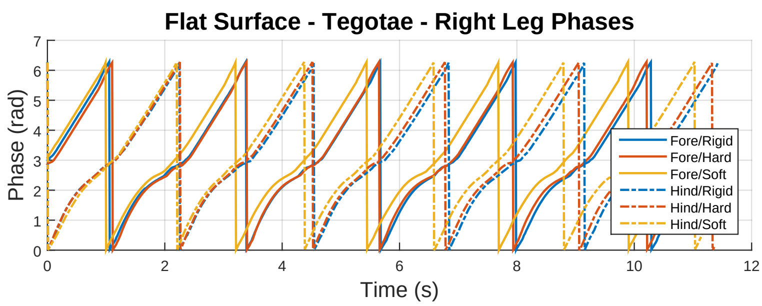

Figure 8. Phase evaluation of fore and hind right limbs when the robot is locomoting on flat surface with Tegotae control. Three different uniform compliance tested. When the limbs are more stiff, the robot-environment interaction is higher and phases get longer delay.

4.5 *Emerging gaits from Tegotae-based control*

Open loop runs were always forced to be trot. However, Tegotae control does not have any direct coupling between phase oscillators of limbs. Nevertheless, on flat surface Tegotae always converges to trot (for our selected $s = 0.3$) no matter which compliant element is used. However, the rough surface has peaks and valleys resulting in unexpected touchdown moments. Even on the rough terrain, the gait mostly remains a trot. But, in some cases deviations from trot have been observed. We believe those deviations towards different gait modes help the robot move more efficiently on the rough terrain. Hence we associate the decrease on the cost of transport (under aforementioned scenarios) to the gait adaptation capability of Tegotae. Indeed, open loop control can sometimes get stuck (repeating same steps blindly with no actual forward motion) on some unfavorable spots on the rough terrain whereas Tegotae control explores different locomotion modes on the same spots and has higher likelihood of passing those points. All of the recorded gait patterns are given in the appendix of this paper.

4.6 *Limitations of the platform:*

Even though it is an animal-like quadruped structure, unlike real animals, legs have proportionally more mass than the body. Moreover, the outer layer of force sensors is covered with rubber which has high friction coefficient which leads to sticktion during the locomotion. The sticktion of force sensors at feet causes energy accumulation in compliant elements during the locomotion. At takeoff, the compliant leg starts oscillating because of the lack of damping. Such oscillations become significant distortions when the leg mass is relatively high compared to the body mass and can be noticed especially in MMBM in the hard case of Fig. 4.

Although Optoforce OMD-30-SE-100N gives 3 axis force information, the readings are well calibrated only when the force is applied on the tip of the sensor dome. During the locomotion the touchdown may occur on any spot of the the sensor and sensor gives less accurate readings when the touchdown point is further away from the tip of the dome. Nevertheless, there are not many commercially available solutions in the market with the similar size and weight. Even though the force measurement may have some numerical errors, their relative response to the changing force is quite acceptable.

5. Conclusions and Future Work

In this paper the effects of leg compliance is investigated. An economical quadrupedal robot is built to test different passive and active compliance characteristics. The robot is a biologically inspired one, but, the morphological characteristics does not strictly imitate any real animal. Instead, it has a modular structure to allow quick morphological changes. Three different passive compliance levels are tested in five different compliance distribution. For each compliance distribution is tested on three different surface (flat, rough and rough/inclined). Furthermore, Tegotae based method is implemented as an active (soft) compliance source and its performance is compared to open loop gait for all proposed scenarios.

Various sensor data has been collected during each trial and later on analyzed based on defined metrics. The problem has many dimensions to consider and there is no single compliance distribution outperforming all the others. Rather there appears to be some favorable combinations for certain criteria in specific scenarios. The relation of compliance to the gait is highly nonlinear and is affected by many parameters. Readers with various different applications in mind can select a subset of findings presented in this paper to guide their compliant robot and controller designs.

Tegotae based control is presenting a great value as an active compliance source. In this study only one level of Tegotae attraction coefficient, s, tested. s is set to a fixed value which has tendency to converge to trot in all test cases. When the limbs are physically more stiff, the effects of Tegotae are more pronounced. One of the most prominent effects of Tegotae is observed to be reducing the cost of transport when locomotion on rough terrain. The most likely reason for such performance increase is the adaptation capability of the Tegotae control. By exploring slight gait changes around trot, it overcomes certain local minima where open loop gaits can exhibit significant performance drops.

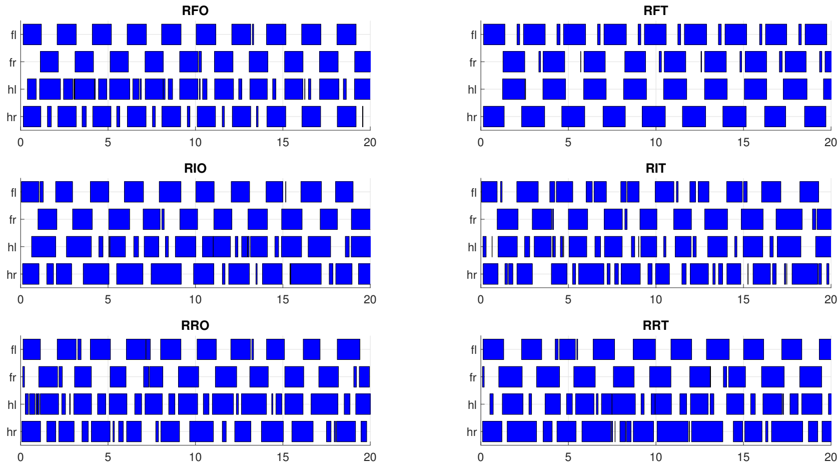

Figure A1. Leg touchdown patterns when all element are rigid.

The open loop gait parameters are optimized with PSO to yield fast and efficient locomotion, so the performance difference between the open loop control and the Tegotae control is not very significant. We expect that Tegotae control has a bigger potential to improve a sub-optimal open loop gait performance. In the future studies, we will include a non-optimal open loop gait to our comparisons to observe if Tegotae would perform proportionally more significant than the open loop control. The feet are completely passive in the current robot. However, feet play a crucial role in locomotion performance too. Our future work will also include integration of active feet to the same platform. Finally, we focused only on a fixed level of Tegotae attraction coefficient, s in this paper. Exploring a wider spectrum of s is also among our future aims.

Acknowledgements

This project is funded by the Swiss National Science Foundation (SNSF) through project number 153299 and the Fundação para a Ciência e a Tecnologia (FCT) agency of Ministry for Education and Science of Portugal with the grant number PD/BD/105781/2014.

Appendix A. Leg touchdown patterns

The leg touchdown is detected by thresholding taking the norm of the force vector obtained from OptoForce sensors. The blue regions in Figs. A1, A2, A3, A4, A5 indicate the foot touchdown and white regions indicate the swing phase. Each plot has a three letter title describing the experiment:

- **1st letter.** R: all rigid elements, H: all hard elements, S: all soft elements, A: fore hard, hind rigid elements, F: fore soft, hind rigid elements,
- **2nd letter.** F: flat surface, R: rough surface, I: rough inclined surface
- **3rd letter.** O: open loop control, T: Tegotae based control

References

[1] Dickinson MH, Farley CT, Full RJ, Koehl MAR, Kram R, Lehman S. How animals move: An integrative view. Science. 2000;288(5463):100–106.
[2] Alexander RM. Elastic energy stores in running vertebrates1. American Zoologist. 1984;24(1):85–94.
[3] Geyer H, Seyfarth A, Blickhan R. Compliant leg behaviour explains basic dynamics of walking and running. Proceedings of the Royal Society B: Biological Sciences. 2006 Nov;273(1603):2861–2867.

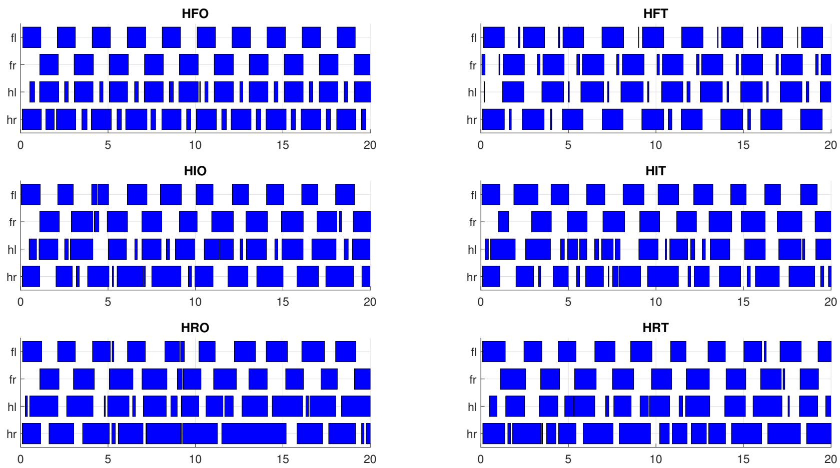

Figure A2. Leg touchdown patterns when all element are hard.

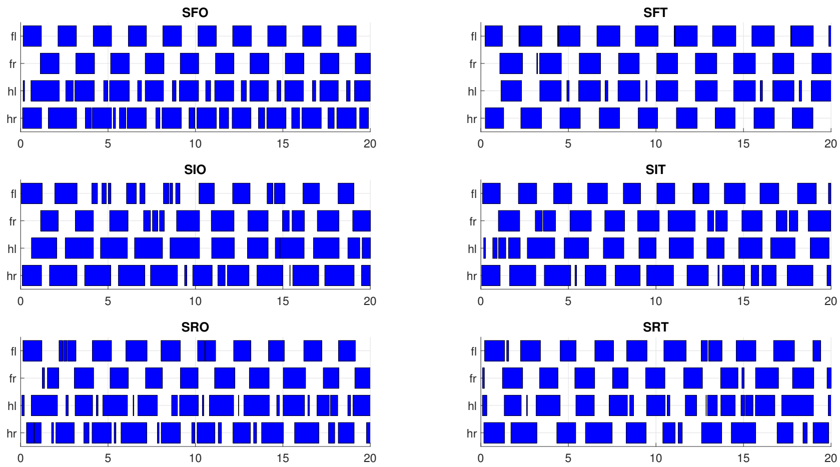

Figure A3. Leg touchdown patterns when all element are soft.

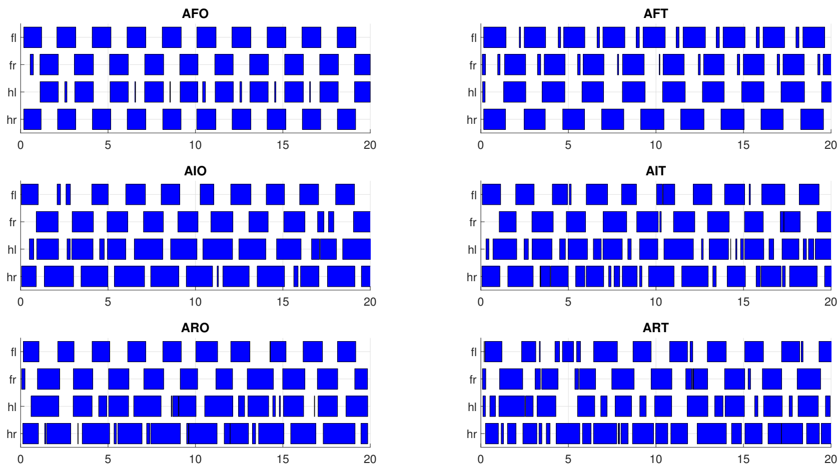

Figure A4. Leg touchdown patterns when fore limb elements are hard and hind limb elements are rigid.

[4] de Lasa M, Buehler M. Dynamic compliant quadruped walking. In: Proceedings 2001 icra. ieee international conference on robotics and automation (cat. no.01ch37164). Vol. 3. 2001. p. 3153–3158 vol.3.

[5] Iida F, Rummel J, Seyfarth A. Bipedal walking and running with compliant legs. In: Proceedings 2007 ieee international conference on robotics and automation. 2007 April. p. 3970–3975.

[6] Hutter M, Remy CD, Hoepflinger MA, Siegwart R. Efficient and versatile locomotion with highly

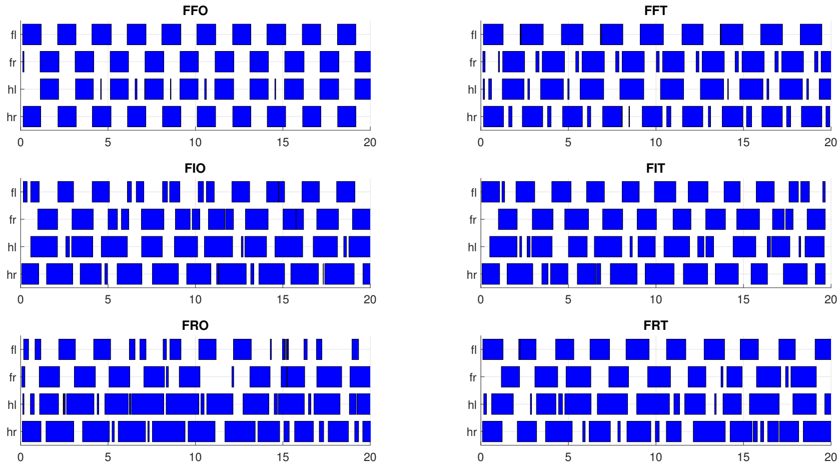

Figure A5. Leg touchdown patterns when fore limb elements are soft and hind limb elements are rigid.

compliant legs. IEEE/ASME Transactions on Mechatronics. 2013 April;18(2):449–458.

[7] Sprwitz A, Tuleu A, Vespignani M, Ajallooeian M, Badri E, Ijspeert AJ. Towards dynamic trot gait locomotion: Design, control, and experiments with cheetah-cub, a compliant quadruped robot. The International Journal of Robotics Research. 2013;32(8):932–950.

[8] Takuma T, Hayashi S, Hosoda K. 3d bipedal robot with tunable leg compliance mechanism for multi-modal locomotion. In: 2008 ieee/rsj international conference on intelligent robots and systems. 2008 Sept. p. 1097–1102.

[9] Hurst JW, Chestnutt JE, Rizzi AA. The actuator with mechanically adjustable series compliance. IEEE Transactions on Robotics. 2010 Aug;26(4):597–606.

[10] Galloway KC, Clark JE, Koditschek DE. Variable Stiffness Legs for Robust, Efficient, and Stable Dynamic Running. Journal of Mechanisms and Robotics. 2013 Jan;5(1):011009–011009–11. Available from: http://dx.doi.org/10.1115/1.4007843.

[11] Kikuuwe R, Yasukouchi S, Fujimoto H, Yamamoto M. Proxy-based sliding mode control: A safer extension of pid position control. IEEE Transactions on Robotics. 2010 Aug;26(4):670–683.

[12] Ajallooeian M, Pouya S, Sproewitz A, Ijspeert AJ. Central pattern generators augmented with virtual model control for quadruped rough terrain locomotion. In: 2013 ieee international conference on robotics and automation. 2013 May. p. 3321–3328.

[13] Focchi M, Boaventura T, Semini C, Frigerio M, Buchli J, Caldwell DG. Torque-control based compliant actuation of a quadruped robot. In: 2012 12th ieee international workshop on advanced motion control (amc). 2012 March. p. 1–6.

[14] Ugurlu B, Kotaka K, Narikiyo T. Actively-compliant locomotion control on rough terrain: Cyclic jumping and trotting experiments on a stiff-by-nature quadruped. In: 2013 ieee international conference on robotics and automation. 2013 May. p. 3313–3320.

[15] Fukuhara A, Owaki D, Kano T, Ishiguro A. Leg stiffness control based on "tegotae" for quadruped locomotion. Cham: Springer International Publishing. 2016. p. 79–84.

[16] Kalakrishnan M, Buchli J, Pastor P, Mistry M, Schaal S. Learning, planning, and control for quadruped locomotion over challenging terrain. The International Journal of Robotics Research. 2011;30(2):236–258.

[17] Buchli J, Kalakrishnan M, Mistry M, Pastor P, Schaal S. Compliant quadruped locomotion over rough terrain. In: 2009 ieee/rsj international conference on intelligent robots and systems. 2009 Oct. p. 814–820.

[18] Owaki D, Goda M, Miyazawa S, Ishiguro A. A minimal model describing hexapedal interlimb coordination: The tegotae-based approach. Frontiers in Neurorobotics. 2017;11:29.

[19] Mutlu M, Hauser S, Berbardino A, Ijspeert AJ. Effects of joint compliance in quadrupedal locomotion. In: The 8th international symposium on adaptive motion of animals and machines. 2017 June.

[20] Vespignani M, Melo K, Mutlu M, Ijspeert AJ. Compliant snake robot locomotion on horizontal pipes. In: 2015 ieee international symposium on safety, security, and rescue robotics (ssrr). 2015 Oct. p. 1–8.

[21] Bramble DM, Lieberman DE. Endurance running and the evolution of Homo. Nature. 2004 Nov;

432:345.
[22] Vasconcelos R, Hauser S, Dzeladini F, Mutlu M, Horvat T, Melo K, Oliveira P, Ijspeert A. Active stabilization of a stiff quadruped robot using local feedback. In: 2017 IEEE/RSJ International Conference on intelligent Robots and Systems (IROS). IEEE. 2017. p. to be updated.
[23] Ijspeert AJ. Central pattern generators for locomotion control in animals and robots: a review. Neural networks. 2008;21(4):642–653.
[24] Collins JJ, Stewart IN. Coupled nonlinear oscillators and the symmetries of animal gaits. Journal of Nonlinear Science. 1993;3(1):349–392.
[25] Cohen AH, Holmes PJ, Rand RH. The nature of the coupling between segmental oscillators of the lamprey spinal generator for locomotion: A mathematical model. Journal of mathematical biology. 1982;13(3):345–369.
[26] Owaki D, Morikawa L, Ishiguro A. Listen to body's message: Quadruped robot that fully exploits physical interaction between legs. In: Intelligent robots and systems (iros), 2012 ieee/rsj international conference on. IEEE. 2012. p. 1950–1955.
[27] Mutlu M, Saranli A, Saranli U. A real-time inertial motion blur metric: Application to frame triggering based motion blur minimization. In: 2014 ieee international conference on robotics and automation (icra). 2014 May. p. 671–676.